1/N Expansion in Correlated Graphene

Valeri N. Kotov,[1] Bruno Uchoa,[2] and A. H. Castro Neto[1]

[1]*Department of Physics, Boston University, 590 Commonwealth Avenue, Boston, Massachusetts 02215*
[2]*Department of Physics, University of Illinois at Urbana-Champaign, Urbana, Illinois 61801*

We examine the $1/N$ expansion, where N is the number of two-component Dirac fermions, for Coulomb interactions in graphene with a gap of magnitude $\Delta = 2m$. We find that for $N\alpha \gg 1$, where α is graphene's "fine structure constant", there is a crossover as a function of distance r from the usual 3D Coulomb law, $V(r) \sim 1/r$, to a 2D Coulomb interaction, $V(r) \sim \ln(N\alpha/mr)$, for $m^{-1} \ll r \ll m^{-1}N\alpha/6$. This effect reflects the weak "confinement" of the electric field in the graphene plane. The crossover also leads to unusual renormalization of the quasiparticle velocity and gap at low momenta. We also discuss the differences between the interaction potential in gapped graphene and usual QED for different coupling regimes.

PACS numbers: 81.05.Uw, 73.43.Cd

I. INTRODUCTION

The physics of graphene, a two-dimensional (2D) allotrope of carbon, presents a unique opportunity to explore properties of gapless (massless) Dirac fermions in a solid-state context[1]. Because graphene is a truly 2D material from electronic point of view, it is also an interesting system where one can explore the important issue of electron-electron interactions. The interaction problem is a central one for the physics of low-dimensional electron systems. Although the electron-electron interactions in graphene are not internally screened, that is, they remain long-range and decay like $1/r$ (the electric field lines propagate in 3D away from the graphene plane and one has the ordinary Coulomb law), there is little experimental evidence, if any, that electron-electron interactions play a role in graphene physics. It is possible that the interactions between the fermions are actually dielectrically screened by the presence of substrates, onto which graphene is deposited in most experimental setups. Nevertheless, there is a fast growing literature in suspended graphene samples[2] that will eventually tell us much more about electron-electron interactions in this amazing material.

In graphene, the strength of the Coulomb interaction relative to the kinetic energy is given by the dimensionless coupling constant (also called graphene's "fine structure constant"),

$$\alpha = \frac{e^2}{\hbar v}, \tag{1}$$

where v is the Fermi velocity, and we absorbed the environmental dielectric constant (ϵ_0) into the definition of the charge e. For graphene in vacuum, as in the case of suspended samples, α reaches its maximum value, $\alpha \approx 2.2$, i.e. interaction effects are expected to be strong. One of the ways strong-coupling effects can manifest themselves theoretically is through spontaneous generation of a mass m (chiral symmetry breaking). In solid state language, mass generation is equivalent to the opening of a gap $\Delta = 2|m|$ in the electronic spectrum. Hence, in this work, the terms "mass" and "gap" are interchangeable. In relativistic quantum electrodynamics (QED) in two space (plus one time) dimensions, QED_{2+1}, the study of this phenomenon started quite a while ago[3,4] and is still going strong today. Graphene is actually different from QED_{2+1} because only the fermions are confined to a 2D plane, while the field lines extend through the whole 3D space. In addition, the Coulomb interaction in graphene can be considered instantaneous since the speed of light c is much larger than the Fermi velocity ($v \approx c/300$). Hence, Lorenz invariance is not respected, which reflects the non-relativistic, purely band origin of the Dirac quasiparticles. For the case of graphene, mass generation has been predicted[5,6], although no experimental signatures have yet been detected. An in-plane magnetic field also favors an excitonic condensate (gap)[7]. There has been a surge of recent numerical activity on the problem of mass generation in graphene (without external field),[8] and a consensus seems to have been reached that above $\alpha_c \approx 1.1$, mass generation occurs[5,8].

Another way to analyze this phenomenon is as a function of N, the number of fermion species, which for graphene is $N = 4$ due to the spin (2) and valley (2) degeneracies. In the strong coupling limit $\alpha \to \infty$, generation of mass occurs below a critical N which was estimated to be $N_c \approx 7 - 9$[5,8]. In experiments, a detectable gap has so far been observed only in a situation when it is actually due to external factors, such as the presence of a substrate with specific symmetry, creating sublattice asymmetry in the graphene plane and thus making the graphene electrons massive (gapped)[9]. However, it is quite possible, as already mentioned, that in "suspended" graphene, whose exploration has just begun, the gap generically exists due to the strong quasiparticle interaction.

Whether graphene breaks overall parity (sublattice symmetry) in the process of spontaneous mass generation depends on the details of the interactions. Long-range Coulomb interactions[5] favor equally parity-even and parity-odd combinations of masses in the two Dirac cones (valleys). On the other hand in QED_{2+1} it is usu-

ally argued that parity-breaking mass generation is not possible, but this has to do with the presence of vector interactions in the fully relativistic model[10].

In this work we study the effect of a finite gap on the quasiparticle interactions (in particular modifications of Coulomb's law), and the renormalization of the quasiparticle parameters, such as the Fermi velocity and the gap itself. Our main goal has been to compute corrections to those quantities under the assumption that the system is already massive, e.g. due to external factors explicitly breaking the sublattice symmetry, as mentioned above. However at the end of the paper we also present estimates how the new physics we find can possibly affect the spontaneous formation of a gap via the excitonic mechanism. We do not address the issue of parity breaking since only single valley Coulomb interactions are considered.

For massless graphene, the large-N limit was studied recently in Refs. [11,12], extending earlier results[13]. The present work can be viewed as an extension of those studies to the massive case. We also find that for massive Dirac fermions unconventional modification of the interaction vertex and fermion's properties can occur, not possible for strictly massless quasiparticles. In particular, we find that there is a crossover regime for $N\alpha \gg 1$ where the 3D Coulomb law, $V(r) \sim 1/r$, is modified, due to the confinement of the electric field lines, to a 2D Coulomb law, $V(r) \sim \ln(1/r)$, with strong renormalizations of the quasiparticle properties. In this non-perturbative regime the photon field is confined to the graphene plane leading to a situation where the Dirac electrons form a 2D "relativistic" Coulomb gas[14]. Such electronic state has never been observed in nature before and, perhaps, with developments in the control of the structure of graphene samples, it can be studied soon.

The paper is organized as follows. In the next section, for completeness, we analyze the weak coupling regime of small α, which can also be relevant to real situations (when the substrate screening is strong). In section III we study the $1/N$ expansion for the electronic properties of gapped Dirac fermions and show the existence of this new intermediate regime where weak confinement of the electric field lines leads to strong renormalization of electron-electron interactions. We also calculate the implications of this new regime in the quasiparticle properties. Section IV contains our conclusions, and in Appendix A some estimates related to the excitonic gap formation are summarized.

II. INTERACTION POTENTIAL: WEAK-COUPLING REGIME

Our starting point is a model of two-dimensional massive Dirac fermions with a gap $\Delta = 2|m|$. The Hamiltonian of the system is[1]

$$H = \sum_{\mathbf{p}} \Psi^\dagger_{\mathbf{p}} (v\boldsymbol{\sigma}\cdot\mathbf{p} \pm m\sigma_3)\Psi_{\mathbf{p}} + H_I, \qquad (2)$$

where H_I is the quasiparticle interaction

$$H_I = \frac{1}{2}\sum_{\mathbf{p}} n_{\mathbf{p}} V(\mathbf{p}) n_{-\mathbf{p}}, \quad n_{\mathbf{p}} \equiv \sum_{\mathbf{q}} \Psi^\dagger_{\mathbf{q}+\mathbf{p}}\Psi_{\mathbf{q}}, \qquad (3)$$

and the potential $V(\mathbf{p})$ will be specified later. We work in a two-component representation, so that $\sigma_i, i = 1,2,3$ are the Pauli matrices; $\hat{\sigma}_0 = \hat{I}$ is the 2×2 identity matrix, often omitted for simplicity, and the vector $\boldsymbol{\sigma} = (\sigma_1, \sigma_2)$. Thus the Hamiltonian (2) describes the physics in a single Dirac cone (valley). The two valleys in graphene are connected by time reversal, which translates into opposite signs of the mass term: the sign " + " in (2) correspond to one of the valleys, while the sign " − " to the other one. All formulas that follow are invariant under a change of the mass sign. The valley (and spin) indexes in (2),(3) are omitted for simplicity, and it is understood that the spinors $\Psi_{\mathbf{q}}$ and the density $n_{\mathbf{p}}$ describe a given single valley.

The low energy electronic spectrum (dispersion close to the Fermi energy), for $H_I = 0$, is given by:

$$E^{\pm}_{\mathbf{k}} = \pm\sqrt{v^2\mathbf{k}^2 + m^2}. \qquad (4)$$

The interaction H_I renormalizes both v and m, as we show later. We will only analyze the case when the system is an insulator, i.e. the chemical potential is in the gap (e.g. fixed to be zero). It is quite remarkable that in recent experiments in gapped samples the chemical potential can actually be moved from the electron to the hole side through the gap, thus causing a metal-insulator transition[15]. In addition to using $\hbar = 1$ everywhere we also put $v = 1$ in all intermediate formulas and restore it only at the end, when necessary.

The polarization function, $\Pi(\mathbf{q},\omega)$, for massive Dirac fermions in the random phase approximation (RPA) was most recently analyzed in detail in Ref. [16] (and can also be deduced by appropriate modification of the Lorentz-invariant results in QED_{2+1}[3]). The result is:

$$\Pi(\mathbf{q},\omega) = -N\frac{|\mathbf{q}|^2}{4\pi}\left\{\frac{m}{q^2} + \frac{1}{2q}\left(1 - \frac{4m^2}{q^2}\right)\arctan\left(\frac{q}{2m}\right)\right\}, \qquad (5)$$

where q is the "3-momentum",

$$q = \sqrt{|\mathbf{q}|^2 - \omega^2}. \qquad (6)$$

In RPA the effective potential is given by:

$$V(\mathbf{q}) = \frac{V^{(0)}_{\mathbf{q}}}{1 - V^{(0)}_{\mathbf{q}}\Pi(q)}, \quad V^{(0)}_{\mathbf{q}} = \frac{2\pi\alpha}{|\mathbf{q}|} \qquad (7)$$

Firstly, we study the behavior of the potential for weak coupling $N\alpha \ll 1$, and in this part of the work we fix N to its graphene value $N = 4$. The first order correction to the static potential is: $\delta V(\mathbf{q}) \approx (V^{(0)}_{\mathbf{q}})^2\Pi(\mathbf{q},\omega = 0)$. After transforming back to real space, we represent the

correction by the function $C(r)$, and write the total potential as

$$V(r) \approx \frac{\alpha}{r}\Big(1 + \alpha C(r) + O(\alpha^2)\Big). \qquad (8)$$

By using (5), we obtain

$$C(r) = -2(mr)\int_0^\infty dx J_0(2mrx) \times \left\{\frac{1}{x} + \left(1 - \frac{1}{x^2}\right)\arctan(x)\right\}, \qquad (9)$$

which is shown in Fig. 1 (lower panel).

At this point we also find it useful to compare our results with the well studied case of conventional QED_{3+1}[17], where interaction effects are also governed by a dimensionless coupling, the fine structure constant α_{QED}. Eq.(8) has the same form (with the substitution $\alpha \to \alpha_{QED} = 1/137$), leading to the so-called Uehling potential. The plot of $C_{QED}(r)$ in this case is shown in Fig. 1 (upper panel)[18]. It should be mentioned that (essentially as a consequence of the uncertainty principle) vacuum polarization effects are expected to be strong only at distances below the Compton wavelength $r < \lambda_C = 1/m$. For our case we find, by evaluating the long distance asymptotic behavior of the integral (9)[19],

$$C(r \gg m^{-1}) \sim -\sqrt{\frac{\pi}{mr}}\, e^{-2mr}\,. \qquad (10)$$

At short distances we find: $C(r \ll m^{-1}) = -\pi/2$, which is the well-known massless limit.

Thus we observe two main differences between massive Dirac fermions and QED: (1) The sign of the correction is different, i.e. in graphene vacuum polarization weakens the potential. This can be traced to the fact that the charge itself e^2 is not renormalized in graphene[16], while it diverges logarithmically at small distances in QED (in other words the distribution of the vacuum polarization charge is very different in the two cases[16]). (2) The magnitude of the correction in graphene is more than 10 times larger (for typical distances), compared to QED (see Fig. 1). This seems to be related to the dimensionality of the problem. Thus, we conclude that (at weak coupling) polarization effects can be appreciable in a wide range of distances, especially if one assumes that Eq.(8) can be used also away from its strict applicability limit $\alpha \ll 1$. Typically such potential modification effects are important for calculation of localized energy levels (in the gap); so far such studies have not been performed experimentally in graphene.

The renormalization of v and m in the weak-coupling regime was addressed in Ref. [16] and will not be repeated here; the main difference from the massless case is that the mass provides an effective infrared cutoff where the renormalization stops, and the mass itself increases logarithmically (to first order in α).

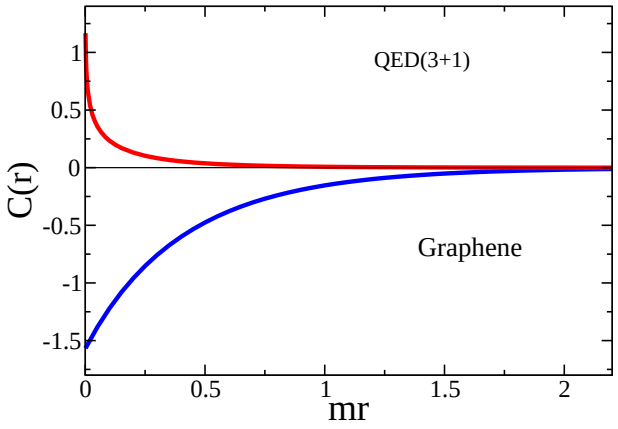

FIG. 1: (Color online.) Plot of $C(r)$ as defined by Eq.(8), for the case of graphene (blue line) and 3D QED (red line).

III. $1/N$ EXPANSION

Now, we analyze the limit $N\alpha \gg 1$, and proceed to evaluate the renormalization of the potential and the quasiparticle properties. We view the calculation as a two-step procedure, which is not exact but will simplify the problem technically: first we calculate divergent terms that originate from intermediate integration in the high momentum region ($m \ll |\mathbf{q}| \ll \Lambda$), where Λ is the ultraviolet cutoff for graphene ($\Lambda \sim 1/a$, where $a \approx 1.42$ Å is the lattice spacing) and after that, as a second step, we concentrate on renormalization from low momenta $|\mathbf{q}| < m$ (such renormalization will be more severe in the strong coupling limit $\alpha \to \infty$).

A. High momentum regime: $m \ll |\mathbf{q}| \ll \Lambda$

To implement the first (large momentum) part of the scheme, one naturally expects the mass term to be unimportant; more formally, we can expand:

$$\Pi(\mathbf{q},\omega) = -\frac{N|\mathbf{q}|^2}{4q}\left\{\frac{1}{4} - \frac{m^2}{q^2} + ...\right\}, \quad q \gg m\,. \qquad (11)$$

Keeping only the first term, one arrives at the effective potential, identical to the one found for the massless case[11,13]:

$$V(\mathbf{q},\omega) \approx \frac{2\pi\alpha}{|\mathbf{q}|}\left\{1 + \frac{\pi g}{8}\frac{|\mathbf{q}|}{q}\right\}^{-1}, \qquad (12)$$

where we use the notation

$$g \equiv N\alpha, \qquad (13)$$

and q is defined by Eq.(6).

Now we evaluate the self-energy correction to one loop, in the limit $g \gg 1$, where the second term in (12) dominates. The self energy is proportional to $1/N$ in this case. The Green's function is

$$\hat{G}^{-1}(\mathbf{k},\omega) = \omega - v\,\boldsymbol{\sigma}\cdot\mathbf{k} - m\,\sigma_3 - \hat{\Sigma}(\mathbf{k},\omega) + i\eta\,\mathrm{sign}(\omega)\,, \qquad (14)$$

where the self-energy at one-loop level is

$$\hat{\Sigma}(\mathbf{k},\omega) = i\int \frac{d^2pd\varepsilon}{(2\pi)^3}\hat{G}_0(\mathbf{k}+\mathbf{p},\omega+\varepsilon)V(\mathbf{p},\varepsilon)\,. \quad (15)$$

Here $\hat{G}_0$ is the free Green's function. By expanding

$$\hat{\Sigma} = \omega\Sigma_0 + v\boldsymbol{\sigma}\cdot\mathbf{k}\Sigma_v + m\sigma_3\Sigma_m\,, \quad (16)$$

we find

$$\hat{G}(\mathbf{k},\omega) = \frac{Z}{\omega - Z(1+\Sigma_v)v\boldsymbol{\sigma}\cdot\mathbf{k} - Zm(1+\Sigma_m)\sigma_3}\,, \quad (17)$$

where Z is the quasiparticle residue:

$$Z^{-1} = 1 - \Sigma_0\,. \quad (18)$$

The calculation of the velocity renormalization is then practically identical to the massless case[11], except one should keep in mind that the mass provides an effective infrared cutoff in the integrals (due to the finite value of the dispersion at zero momentum (4)). Thus we put the mass to zero to avoid lengthy formulas and keep the above in mind. One finally obtains ($\delta v(k)$ stands for the velocity correction at one-loop order)

$$\frac{\delta v(k)}{v} = \Sigma_0 + \Sigma_v = -i\frac{16}{N}\int_k^\Lambda \frac{pdp}{(2\pi)}\int_{-\infty}^{\infty}\frac{d\omega}{(2\pi)}(p^2-\omega^2)^{-3/2}, \quad (19)$$

where k is the external momentum (neglected in the Green's function), and written as an effective infrared cutoff (thus we assume $k \gg m$; in the opposite limit m is the cutoff). By performing Wick's rotation $\omega \to i\omega$ (which avoids crossing any poles)[17], one finds

$$\delta v(k)/v = \frac{8}{\pi^2}\frac{1}{N}\ln(\Lambda/k), \quad m \ll k \ll \Lambda\,. \quad (20)$$

As expected, the result is this region is identical to the massless case[11].

For the mass renormalization we have, written in more detail,

$$\frac{\delta m(k)}{m} = \Sigma_0 + \Sigma_m = -i\frac{16}{N}\int_k^\Lambda \frac{pdp}{(2\pi)}\int\frac{d\omega}{(2\pi)}\frac{\sqrt{p^2-\omega^2}}{p^2} \times\left\{\frac{p^2+\omega^2}{(p^2-\omega^2)^2} + \frac{1}{p^2-\omega^2}\right\}. \quad (21)$$

Here the first term in the curly brackets corresponds to Σ_0 and the second one to Σ_m. The final result is

$$\delta m(k)/m = \frac{16}{\pi^2}\frac{1}{N}\ln(\Lambda/k), \quad m \ll k \ll \Lambda\,. \quad (22)$$

Finally, the quasiparticle residue Z is determined by the behavior of Σ_0. However in the limit $g \gg 1$ one encounters some complications, because even the frequency integral in the expression for Σ_0 (see (21)) is logarithmically divergent (although in the sum $\Sigma_0 + \Sigma_m$ this additional divergence is not present). This means that we have to use the full, finite g potential from (12). Performing the calculation one finds

$$\Sigma_0 = \frac{\alpha}{\pi}\ln(\Lambda/k)\int_0^\infty dx\frac{1-x^2}{(g\pi/8+\sqrt{1+x^2})(1+x^2)^{3/2}}\,, \quad (23)$$

and therefore,

$$Z \approx 1 - \frac{8}{\pi^2}\frac{1}{N}\ln(g\pi/4)\ln(\Lambda/k),\ g \gg 1,\ m \ll k \ll \Lambda\,. \quad (24)$$

The results for the mass and velocity renormalization (20), (22) can be used to form renormalization group (RG) equations for these quantities. The reasoning is similar to the one presented, for example, in ref.[11] for the massless case. One integrates out the high momentum degrees of freedom, i.e. momentum regions $\Lambda > |\mathbf{p}| > \Lambda_1$, and the results vary with the quantity $\ln(\Lambda/\Lambda_1) \equiv l$. As evident from (20) and (22) the renormalization should stop at a scale $\sim m$. For m large enough and $N\alpha \gg 1$, the functional form of the potential (12) is not significantly affected by the RG flow before it stops. The RG equations in that case are:

$$\frac{dv}{dl} = \frac{8}{N\pi^2}v\,, \qquad \frac{dm}{dl} = \frac{16}{N\pi^2}m\,, \quad (25)$$

that have the solutions:

$$m(k) = m\left(\frac{\Lambda}{k}\right)^{\frac{16}{N\pi^2}}, \quad v(k) = v\left(\frac{\Lambda}{k}\right)^{\frac{8}{N\pi^2}}, \quad (26)$$

which are valid in the region $m \ll k \ll \Lambda$. Here m, v are the corresponding quantities at the ultraviolet scale Λ, i.e. their initial band values at the lattice scale.

B. Low-momentum regime: $|\mathbf{q}| \ll m$

Now we proceed to analyze the low-momentum region. In this limit, the polarization (5) can be expanded to give:

$$\Pi(\mathbf{q},\omega) = -\frac{N|\mathbf{q}|^2}{12\pi m}\left\{1 - \frac{q^2}{10m^2} + ...\right\}, \quad q \ll m\,. \quad (27)$$

We keep only the first term, as the other terms decrease quite fast in powers of q/m. Notice also that in this limit $\Pi(\mathbf{q},\omega)$ becomes frequency independent. The corresponding RPA effective potential is:

$$V(\mathbf{q}) \approx \frac{2\pi\alpha}{|\mathbf{q}| + \tilde{g}|\mathbf{q}|^2/m}\,, \quad |\mathbf{q}| \lesssim m\,, \quad (28)$$

where we have defined:

$$\tilde{g} \equiv g/6 = N\alpha/6\,. \quad (29)$$

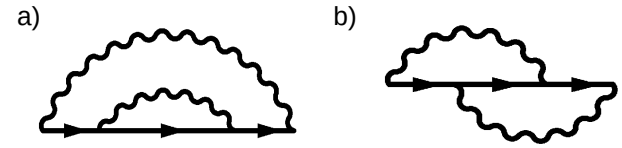

FIG. 2: Two diagrams contributing to the self-energy at two-loop level. The wavy line stands for the potential (28).

By direct numerical evaluation of the polarization bubble[16], we actually find that the above formula is valid even up to $|\mathbf{q}| \sim m$.

In the strict long-distance limit $|\mathbf{q}| \to 0$ the above potential tends to the pure Coulomb potential. However, in the limit $\tilde{g} \to \infty$ there is an intermediate window of momenta, $m/\tilde{g} \ll |\mathbf{q}| < m$, where the potential crosses over to the 2D Coulomb's law,

$$V(\mathbf{q}) \approx \frac{12\pi m}{N}\frac{1}{|\mathbf{q}|^2}, \quad m/\tilde{g} \ll |\mathbf{q}| < m. \tag{30}$$

In real space we have:

$$V(r) \approx \frac{6}{N} m \ln\left(\frac{\tilde{g}}{mr}\right), \quad \frac{\tilde{g}}{m} \gg r \gg \frac{1}{m}. \tag{31}$$

We also comment on some other situations in electrodynamics when the Coulomb potential can be strongly modified. It is known that in compact QED_{2+1} linear confinement can occur due to non-perturbative instanton effects[20]. It is also possible to have a confining potential in ferroelectrics where compact field configurations are favored leading to linear confinement of charges[21]. Intermediate logarithmic behavior (in real space), similar to (31), can occur in thin films (of thickness d) with large dielectric constant $\kappa \gg 1$[22]. In that case the logarithmic behavior is limited to the region: $d \ll r \ll \kappa d$, i.e. d plays the role (formally) of the "Compton" wavelength $1/m$ in our case, and κd plays the role of $N\alpha/m$. It was argued that such an intermediate regime can actually lead to modification of the variable-range-hopping law in systems with strong disorder. Finally, a mechanism similar to the one found in this work, i.e. due to the dominance of fluctuations over the bare potential, was explored in the context of high temperature superconductivity models based on QED (where it contributes to spinon deconfinement-confinement transition)[23].

Now we show that the low-momentum region where (28) is valid, also contributes singularly to the self-energy, in the strong-coupling limit $\alpha \gg 1$. Using again the expression (15) with the potential (28), we obtain for the velocity renormalization at one-loop level,

$$\frac{\delta v^{(1)}(k)}{v} = i\int_k^m \frac{pdp}{(2\pi)}\int\frac{d\omega}{(2\pi)}\frac{1}{\omega^2 - m^2}V(|\mathbf{p}|)\,. \tag{32}$$

Here we have put the fermion energies $E_{\mathbf{p}} \approx m$. Because the potential is static, there is no residue renormalization ($Z = 1$) in this momentum range, and we have finally

$$\frac{\delta v^{(1)}(k)}{v} = \frac{3}{N}\ln\left(\frac{1+\tilde{g}}{1+\tilde{g}k/m}\right) \approx \frac{3}{N}\ln(m/k), \quad m/\tilde{g} \ll k \ll m\,. \tag{33}$$

Performing the same calculation for the mass, one easily finds

$$\delta m^{(1)}(k)/m = \delta v^{(1)}(k)/v\,. \tag{34}$$

Let us also examine the two-loop self-energy which is given by the two diagrams of Fig. 2. After some rather involved calculations we obtain the first, "rainbow" contribution (Fig. 2(a))

$$\hat{\Sigma}_a^{(2)} = -\frac{1}{N^2}\Big(\frac{9}{2}v\boldsymbol{\sigma}\cdot\mathbf{k} + \frac{9}{4}m\sigma_3\Big)\ln(m/k)\,, \tag{35}$$

in the low-momentum region $m/\tilde{g} \ll k \ll m$. For the vertex correction to the self-energy, shown in Fig. 2(b), we find:

$$\hat{\Sigma}_b^{(2)} = -\frac{1}{N^2}\big(\omega + 3v\boldsymbol{\sigma}\cdot\mathbf{k} + 3m\sigma_3\big)\ln(m/k)\,. \tag{36}$$

From here we find the corrections to v, m, Z at this order:

$$\begin{aligned}\frac{\delta v^{(2)}}{v} &= -\frac{17}{2}\frac{1}{N^2}\ln(m/k)\,,\\ \frac{\delta m^{(2)}}{m} &= -\frac{25}{4}\frac{1}{N^2}\ln(m/k)\,,\\ Z^{(2)} &\approx 1 - \frac{1}{N^2}\ln(m/k)\,,\end{aligned} \tag{37}$$

valid for $m/\tilde{g} \ll k \ll m$.

Observe that a single logarithm appears at two loops, meaning that we do not have a conventional renormalization group situation (piling up of leading logs) in this low-momentum region. This behavior is similar to the case of a static Coulomb potential in the massless case, where a single log appears up to second order of perturbation theory[24].

Let m^*, v^* be the values of these quantities at the lowest scale $k \sim m/\tilde{g} \ll m$. Keeping only the dominant one loop contribution, we can estimate

$$v^*/v = m^*/m \approx 1 + \frac{3}{N}\ln(\tilde{g}) + O(1/N^2)\,. \tag{38}$$

From equations (4),(38) one can also deduce the correction to the dispersion at low momenta:

$$|E_k| \approx m^* + \frac{(v^*)^2k^2}{2m^*} \approx \left(1 + \frac{3}{N}\ln(\tilde{g})\right)\left(m + \frac{v^2k^2}{2m}\right), \tag{39}$$

for $k \sim m/\tilde{g} \ll m$.

On the validity of the above expansions, comparing Eq. (33) and (37) we note that in two loop the $1/N$ expansion breaks down for $N \approx N_c = 17/6$, when the coefficient in front of the log vanishes and the trend in

the renormalization of the velocity is reversed towards increasing α. In the strong coupling limit, $\alpha \to \infty$, the velocity renormalizes to zero, reinforcing α to be large, what indicates the possibility of an instability below the critical N. Although this analysis is not directly applicable to graphene, where $N = 4$, it is similar in spirit to the prediction of a metal-insulator transition in massless graphene[5,8], which would take place around the critical value $\alpha_c \approx 1$, where usual perturbation theory in the Coulomb potential breaks down.

In this regard it is also important to explore how the change in the potential, leading to the modified shape (30), can affect the spontaneous formation of a mass gap via the non-perturbative excitonic mechanism[5,6]. The complete self-consistent examination of this problem is well beyond the scope of this work[25]; however some estimates are presented in Appendix A. We can conclude (see Eq. (A3)) that the gap increases as $\tilde{g}$ increases,

$$m \approx \Lambda e^{-\pi N/4 + (3\pi/4)\ln(\tilde{g})} = \Lambda \tilde{g}^{(3\pi/4)} e^{-\pi N/4} , \qquad (40)$$

although this increase in small in the perturbative $1/N$ regime when $\ln(\tilde{g})/N \ll 1$. On the other hand when

$$\frac{3}{N}\ln(\tilde{g}) \sim 1 , \qquad (41)$$

the gap enhancement is substantial. However this strong-coupling regime in not accessible within the conventional large N philosophy, where $\tilde{g} = N\alpha/6$ is kept fixed while $N \gg 1$, so that the RPA self-consistent scheme is well justified. One can also hope that the results represent correctly the behavior for N fixed at its physical value ($N = 4$) with $\tilde{g}$ large at strong coupling ($\alpha \gg 1$), but of course in this case diagrams beyond RPA might be important and their influence remains unclear. Therefore we cannot make a definite conclusion how the system behaves under the condition $\frac{3}{N}\ln(\tilde{g}) \sim 1$, although on the surface of things this criterion signifies a transition into a new low-energy regime which in itself deserves further study.

IV. CONCLUSIONS

In conclusion, we have studied the behavior of the interaction potential and the quasiparticle properties both in the weak-coupling $g = N\alpha \ll 1$ and the "strong-coupling" $g = N\alpha \gg 1$ regimes. In the latter case we have found an unconventional regime where the potential crosses over from the usual 3D Coulomb potential to a 2D logarithmic behavior, as if the field lines were confined in the plane. This is due to the fact that vacuum fluctuations dominate over the bare potential, although they do so in a limited momentum range. This physics can also lead to unusual renormalization of physical quantities at distances well beyond the Compton wavelength $1/m$ (i.e. momenta $q \ll m$), up to distances of order $g/m \gg 1/m$. Such effects have not been studied, to the best of our knowledge, in conventional QED due to the smallness of α_{QED}. In our case both the mass gap and the velocity "keep running" (increase) up to the larger distance g/m. Since for graphene in vacuum $g \approx 9$, one can hope that this physics is observable. On the other hand, the presence of various numerical coefficients makes this somewhat difficult, e.g. in (31) $\tilde{g} = g/6 = 1.5$ is probably too small to create a large-enough intermediate energy window. Nevertheless, from purely theoretical perspective, the massive case exhibits much richer behavior compared to the gapless one.

Acknowledgments

We are grateful to R. Barankov, E. Fradkin, E. Marino, V. Pereira, and O. Sushkov for many stimulating discussions. We thank Roman Barankov for showing us the derivation of Eq. (10). This work was supported in part by the Office of Science, U.S. Department of Energy under Contract DE-FG02-91ER45439 through the Frederick Seitz Materials Research Laboratory at the University of Illinois. AHCN acknowledges the partial support of the U.S. Department of Energy under the grant DE-FG02-08ER46512.

APPENDIX A: ENHANCEMENT OF EXCITONIC INSTABILITY DUE TO COULOMB'S LAW MODIFICATION AT STRONG COUPLING

The equation for excitonic pairing leading to generation of mass m can be derived by determining the self-energy in Eq. (15) self-consistently, i.e. substituting $\hat{G}_0 \to \hat{G}$ in that equation. Even if the "bare" mass is initially zero, a finite (momentum-dependent) mass is then non-perturbatively generated, and obeys the equation:

$$m(0) = \frac{1}{2}\int \frac{d^2k}{(2\pi)^2} \frac{V(|\mathbf{k}|)m(k)}{\sqrt{k^2 + m(k)^2}}. \qquad (A1)$$

In the gap equation vertex corrections are ignored (in the spirit of the large N approach), and the static limit of the RPA potential $V(|\mathbf{k}|$ is often used[6]. Naturally, if on the right-hand side the mass $m(k) = m$ were the non-zero mass already present in the Hamiltonian, then the above equation would simply be the first perturbative correction to the mass, discussed in Section III.

It is known that the momentum dependence of the mass cannot be ignored, and is important down to momenta $k \sim m(0)$ when the solution levels off. The full analysis results in the presence of a critical N, below which the solution exists[4,6]. However, in order to estimate the influence of the potential (30) on the gap, we use a simplified approach which misses the existence of a critical coupling, but provides a good qualitative estimate (and is similar to the initial attacks on the problem of chiral symmetry breaking[3]). This approach amounts

to ignoring the momentum dependence of the mass, and we then obtain:

$$m \approx \int_m^\Lambda \frac{kdk}{4\pi}\left(\frac{16}{Nk}\right)\frac{m}{|E^\pm_{\mathbf{k}}|} + \int_{m/\tilde{g}}^m \frac{kdk}{4\pi}\left(\frac{12\pi m}{Nk^2}\right)\frac{m}{|E^\pm_{\mathbf{k}}|}. \quad \text{(A2)}$$

Here $E^\pm_{\mathbf{k}}$ is given by (4), and in our units $v = 1$. The interaction potential in the above equation is taken in the limit $g \gg 1$, and we have taken into account the fact that the potential shape depends on the momentum range, as determined by Eqs. (12),(30). From here we find the solution

$$m \approx \Lambda e^{-\pi N/4 + (3\pi/4)\ln(\tilde{g})} = \Lambda \tilde{g}^{(3\pi/4)} e^{-\pi N/4}. \quad \text{(A3)}$$

It is clear that in the regime $\ln(\tilde{g})/N \ll 1$ we have an exponentially small solution. Only when $\frac{3}{N}\ln(\tilde{g}) \sim 1$, a substantial enhancement of the excitonic gap is possible, i.e. the exponential dependence disappears, and the gap is proportional to the large cutoff scale Λ. The condition $\frac{3}{N}\ln(\tilde{g}) \sim 1$ marks, as expected, a transition to a non-perturbative regime, where the perturbative $1/N$ corrections previously computed (see Eq. (38)) become large, and the $1/N$ expansion breaks down.

[1] A. H. Castro Neto, F. Guinea, N. M. R. Peres, K. S. Novoselov, and A. K. Geim, Rev. Mod. Phys. **81**, 109 (2009).

[2] K. I. Bolotin, K. J. Sikes, Z. Jiang, M. Klima, G. Fudenberg, J. Hone, P. Kim, and H. L. Stormer, Solid State Communications **146**, 351 (2008); X. Du, I. Skachko, A. Barker, and E. Y. Andrei, Nature Nanotechnology **3**, 491 (2008).

[3] R. D. Pisarski, Phys. Rev. D **29**, 2423 (1984); T. W. Appelquist, M. Bowick, D. Karabali, and L. C. R. Wijewardhana, Phys. Rev. D **33**, 3704 (1986).

[4] T. Appelquist, D. Nash, and L. C. R. Wijewardhana, Phys. Rev. Lett. **60**, 2575 (1988).

[5] D. V. Khveshchenko, J. Phys.: Condens. Matter **21**, 075303 (2009), and cited references.

[6] D. V. Khveshchenko, Phys. Rev. Lett. **87**, 246802 (2001); D. V. Khveshchenko and H. Leal, Nucl. Phys. B **687**, 323 (2004).

[7] I. L. Aleiner, D. E. Kharzeev, and A. M. Tsvelik, Phys. Rev. B **76**, 195415 (2007).

[8] J. E. Drut and T. A. Lahde, Phys. Rev. Lett. **102**, 026802 (2009); J. E. Drut and T. A. Lahde, Phys. Rev. B **79**, 165425 (2009); S. Hands and C. Strouthos, Phys. Rev. B **78**, 165423 (2008); G.-Z. Liu, W. Li, and G. Cheng, Phys. Rev. B **79**, 205429 (2009).

[9] S. Y. Zhou, G.-H. Gweon, A.V. Fedorov, P.N. First, W.A. de Heer, D.-H. Lee, F. Guinea, A.H. Castro Neto, and A. Lanzara, Nature Materials **6**, 770 (2007).

[10] T. Appelquist, M. Bowick, D. Karabali, and L. C. R. Wijewardhana, Phys. Rev. D **33**, 3774 (1986).

[11] D. T. Son, Phys. Rev. B **75**, 235423 (2007).

[12] M. S. Foster and I. L. Aleiner, Phys. Rev. B **77**, 195413 (2008).

[13] J. González, F. Guinea, and M. A. H. Vozmediano, Phys. Rev. B **59**, R2474 (1999).

[14] E. C. Marino, Nucl. Phys. B **408**, 551 (1993), R. D. Pisarski, Phys. Rev. D **29**, 2423 (1984).

[15] S. Y. Zhou, D. A. Siegel, A. V. Fedorov, and A. Lanzara, Phys. Rev. Lett. **101**, 086402 (2008).

[16] V. N. Kotov, V. M. Pereira, and B. Uchoa, Phys. Rev. B **78**, 075433 (2008).

[17] V. B. Berestetskii, E. M. Lifshitz, and L. P. Pitaevskii, *Quantum Electrodynamics*, (Pergamon, Oxford, 1982).

[18] In conventional (3+1 dimensional) QED we have[17]: $C_{QED}(r) = 2/(3\pi)\int_0^\infty dx\; e^{-2mrx}\left[1+(2x)^{-2}\right]x^{-2}\sqrt{x^2-1}$, and $C_{QED}(r) \sim (4\sqrt{\pi})^{-1}(mr)^{-3/2}\; e^{-2mr}, mr \gg 1$.

[19] We are grateful to Roman Barankov for showing us the derivation of the asymptotic expansion.

[20] A. M. Polyakov, *Gauge Fields and Strings*, (Harwood Academic Publishers, Chur, 1987).

[21] D. A. Kirzhnits and M. A. Mikaelyan, JETP Lett. **39**, 701 (1984); JETP **97**, 795 (1990).

[22] B. I. Shklovskii, arXiv:0803.3331.

[23] D. H. Kim and P. A. Lee, Annals of Physics, **272**, 130 (1999); Z. Tesanovic, O. Vafek, and M. Franz, Phys. Rev. B **65**, 180511 (2002); I. F. Herbut, Phys. Rev. B **66**, 094504 (2002).

[24] E. G. Mishchenko, Phys. Rev. Lett. **98**, 216801 (2007); O. Vafek and M. J. Case, Phys. Rev. B **77**, 033410 (2008).

[25] The fact that in our model the generated mass also determines a confinement energy scale resembles to an extent the behavior of $2+1$ dimensional quantum chromodynamics, see e.g. T. Appelquist and D. Nash, Phys. Rev. Lett. **64**, 721 (1990).